5

Analysis of Human Fibroblasts by Atomic Force Microscopy

Gillian R. Bushell, Colm Cahill, Sverre Myhra, and Gregory S. Watson

1. Introduction

The force-sensing members of the large family of scanning probe microscopies have become important tools during the past decade for visualizing, characterizing, and manipulating objects and processes on the meso- and nanoscale level. The atomic force microscope (AFM), in particular, has had an impact in the life sciences. In cell science, the pioneering work with AFM was conducted in the early 1990s ***(1–3)***. The methodologies have now reached a stage of relative maturity ***(4)***. The principal merit of the AFM is as a nonintrusive local probe of live cells and their dynamics in the biofluid environment. As well as offering high spatial resolution imaging in one or more operational modes, the AFM can deliver characterization of mechanical properties and local chemistry through operation in the force-vs-distance (F-d) mode (e.g., **ref. *5***). The lateral resolution delivered by the AFM will in most cases, and especially for soft materials, be inferior to that obtained by electron-optical techniques, but the *z*-resolution is routinely in the nanometer range with a depth of focus equal to the dynamic range of the *z*-stage travel. The instrument may be operated in one of several modes, of which the most common ones are as follows: the contact mode, using a soft lever in which contours of constant strength of interaction are traced out; the intermittent-contact mode, in which a relatively stiff lever is vibrated at a frequency near that of a free-running resonance and in which contours of constant decrement of the free-running amplitude or a constant phase shift are mapped; and the F-d mode, in which the local stiffness of interaction between tip and specimen is determined over a range of applied force (lever deflection and *z*-stage travel being the two measurable variables).

From: *Methods in Molecular Biology, vol. 242: Atomic Force Microscopy: Biomedical Methods and Applications*
Edited by: P. C. Braga and D. Ricci © Humana Press Inc., Totowa, NJ

2. Materials

2.1. Cell Culture: Handling and Preparation for In Vitro Analysis by AFM

Primary human skin fibroblasts and 3T3 cells are generally maintained as monolayer cultures in Dulbecco's modified Eagles' medium/Ham F12 containing 15 m*M* $NaHCO_3$, 50 U/mL penicillin, 50 mg/mL streptomycin, and supplemented with 10% inactivated (by heat) fetal calf serum (FCS). The cultures are then grown in a humidified environment with a 5% CO_2 atmosphere at 37°C. There are two reliable methods for preparation of live cells for AFM analysis.

2.1.1. Live Cells—Method 1

The cells are harvested by trypsin treatment in preparation for AFM analysis and are then grown overnight on sterile untreated glass cover slips. The cover slips are washed five times with serum free media (Dulbecco's modified Eagles' medium/Ham F12) containing 20 m*M* HEPES at pH 7.3. The cover slips can then be attached to standard AFM mounting plates before being covered with a droplet of fluid, in anticipation of in vitro analysis.

2.1.2. Live Cells—Method 2

The cells are grown overnight in sterile tissue culture dishes 150- or 40-mm diameter (e.g., Corning, cat. no. 430599). The preferred dishes have been pretreated by the manufacturer so as to present a negatively charged and hydrophilic surface and thus ensure better cell adherence. The cells are then washed, as in the previous paragraph, and covered to a depth of 2–3 mm with serum-free media.

2.1.3. Fixed Cells

The preparation follows a modified procedure of Pietrasanta et al. ***(6)***.

The cells on cover slips are washed for 1 min in prewarmed (37°C) phosphate-buffered saline (PBS), and then for another 1 min in stabilizing S-buffer (0.1 *M* PIPES, pH 6.9, 0.5 m*M* $MgCl_2$, and 0.1 m*M* ethylenediamine tetraacetic acid). After stabilization the cover slips are washed again in PBS before fixing in 0.01% gluteraldehyde (in S buffer) for 10 min. This is followed by another wash in PBS before being thoroughly rinsed in deionized and distilled water. Finally, the specimens are dehydrated with ethanol (70, 80, 90, and 100% in sequence for 5 min per step). The specimens are then allowed to dry in air, whereupon they are ready for AFM analysis.

2.1.4. Dehydrated Cells

The preparatory sequence is identical to that described in the introductory paragraph. However, instead of placing the cultures in a biocompatible liquid for analysis, they are now rinsed to remove excess salts, allowed to dry in air for 30 min or more, and then investigated by AFM over periods up to 3 h. In some cases, it may be possible to continue analysis for periods up to 48 h.

2.2. AFM Instrumentation and Methodology

1. Instrumentation. The examples of AFM analyses described in **Subheading 3.** were performed with a ThermoMicroscope TMX-2000 multitechnique scanning probe microscopy system. Some of the results were obtained with a Discoverer Stage attachment using an open fluid cell defined by a droplet of water trapped between the glass window on the detector stage and the cover slip substrate (similar to that described in **ref. *3***. In this configuration, a 70×70 μm^2 scanner with a z range of some 13 μm was used. Any one of the mainstream AFM instruments will offer a comparable facility. On other occasions, an Explorer Stage attachment provided increased flexibility and convenience. Again, an open cell could be defined by a trapped droplet as in the case of the Discoverer Stage. It is preferable to grow the cell culture directly in a culture dish that will then constitute the fluid cell for the Explorer Stage. Several of the AFM manufacturers now offer comparably equipped standalone instruments or equivalent optional attachments. The preferred scanner for the latter procedure should have a maximum field of view of some 130×130 μm^2 and a z range of 10 μm. All combinations of instrumentation will accommodate the full range of relevant operational modes: contact, *in situ* intermittent-contact in fluid, and F-d analysis.
2. Probe. A range of probes, available from several suppliers, can be used for contact-mode imaging and F-d analysis. Live cells, especially the plasma membrane, are soft objects in the context of AFM analysis (with an effective Young's modulus of less than 1 MPa). Accordingly it is necessary to work with a lever with a spring constant, k_N, in the range 0.001–0.1 N/m to avoid excessive tip indentation. The lower end of that range is suitable for general imaging and F-d analysis of the unsupported plasma membrane, whereas the upper end may be used for imaging the harder elements of the intracellular and cytoskeletal structures. Typical choices include (1) a V-shaped Si_3N_4 lever, with integral square pyramidal tip (nominal radius of curvature, R_{tip} = 40 nm, and aspect ratio, A_r. = 0.7), and with nominal values for k_N of 0.03 and 0.06 N/m; (2) a V-shaped lever, with integral triangular pyramidal tips with smaller tip radii (R_{tip} = 10–20 nm), and greater aspect ratio (A_r = 3), and with k_N = 0.5 N/m. The actual spring constant for a particular lever can be calibrated in anticipation of F-d analysis in accord with a method described in the literature ***(7)***. Other methods will offer similar information ***(8)***.

3. Methods

3.1. Fluid Ambient Environment

3.1.1. Maintenance of Static Conditions

The principal variables requiring control are temperature and fluid volume. If the fluid cell is defined by a trapped droplet, then frequent replenishment of the reservoir is required. Thus, imaging conditions will need to be reestablished at regular intervals (typically 30 min), but there is then opportunity also to reestablish optimum temperature. A larger fluid cell, such as a culture dish, with a volume of some 5 mL or more, will have a longer life span with respect to evaporative losses, and the greater thermal inertia will promote temperature stability. However, long-term stability over some hours will require replenishment. The optimum temperature can then be reestablished by total replacement of the media. Although flow-through replacement from an external reservoir is another option, the imaging conditions are likely then to be affected when a soft lever is being used. Another alternative is that of continuous heating of the cell by a hot stage, the disadvantages then being associated with thermal contraction/expansion and with thermal convection currents in the fluid.

3.1.2. Injection of Reactants for Dynamic Studies

When slow dynamics are being investigated, reactants may be introduced when there is replenishment or replacement of media. A practiced operator can usually reestablish imaging/analysis conditions within a few minutes. More rapid injection and mixing is required if fast dynamics are being investigated. Access to the fluid cell is generally restricted by the compact design of most instruments. Accordingly, a flow-through cell arrangement may be the better choice when interruption of the imaging conditions cannot be tolerated or when a particular field of view needs to be tracked continuously.

3.2. AFM Imaging and F-d Analysis

3.2.1.Imaging of Cells

3.2.1.1. Fixed or Dehydrated Cells

When a cell is fixed, through cross-linking of the plasma membrane and/or dehydration, it becomes a hard object. Consequently, it can be imaged in air by routine AFM procedures; a typical contact mode image of a fixed cell is shown in **Fig. 1**. However, scanning electron microscopy (SEM)/tunnelling electron microscopy (TEM) are richer sources of information and are generally to be preferred for this type of investigation.

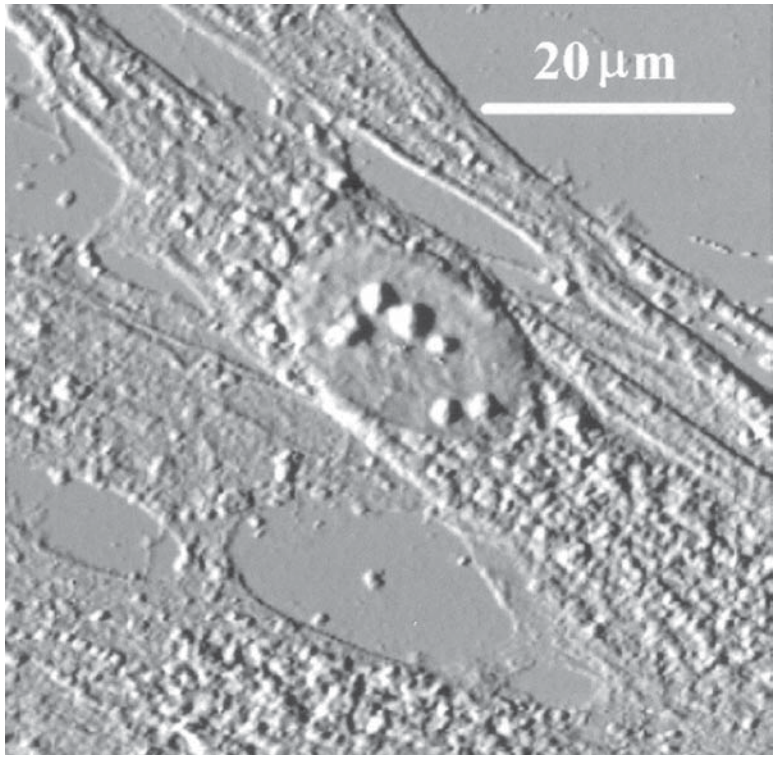

Fig. 1 Example of a fixed fibroblast imaged in air in the contact mode.

3.2.1.2. Live Cells In Vitro

Live cells on untreated cover slips rarely produce acceptable contact mode images because of poor adherence to the substrate, gross fouling of the tip, and destructive tip–membrane interactions (*see* **Notes 1–3**).

However, cells grown on surface-treated culture dishes offer greatly improved imaging conditions. Continuous scanning at linear scan speeds of 150 µm/s and at force loads in the low-nN range can now be conducted over several hours without any apparent damage to viable cells. A typical example of a contact mode image of a lamellipodial region of a fibroblast is shown in **Fig. 2**; the contour line reveals intracellular structure with a *z* resolution in the low-nm range.

3.2.2. Intermittent-Contact Resonance Mode Imaging

It is argued that the intermittent-contact resonance mode (also known as tapping mode) will result in better image quality for soft specimens. The mode

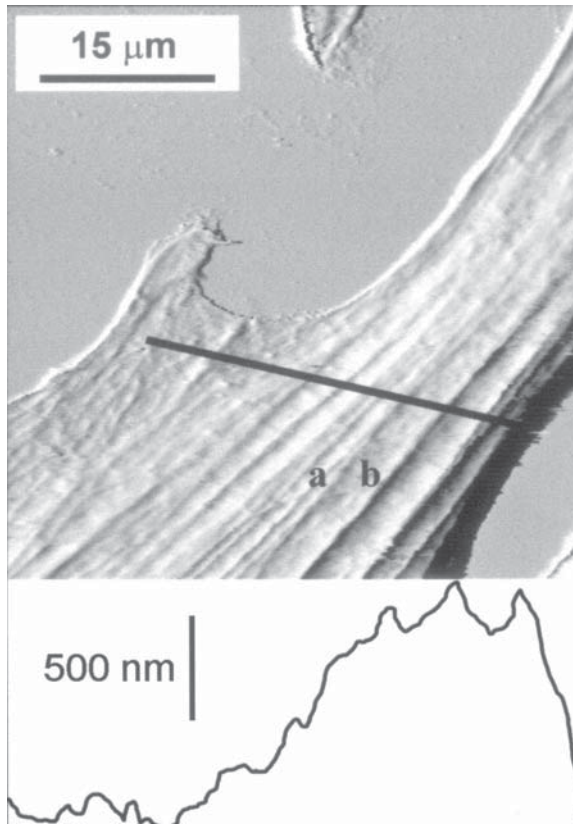

Fig. 2 Lamellipodial region of a live human fibroblast in its biocompatible fluid medium on a culture dish substrate. Contact mode imaging was performed with a standard probe having a pyramidal tip (radius of curvature of 40 nm) and a lever spring constant k_N = 0.03 N/m. The lever-imposed force loading was approx 3 nN and the fast-scan speed was 150 μm/s. The contour line reveals submembrane structure.

has two distinct advantages. The effect of lateral forces is effectively eliminated (important because cells have low resistance to shear stress). Because the interaction now arises from an impulse action at one extreme of the oscillatory motion of the tip, the inertia of the sample will resist deformation. However, the resolution of resonance mode imaging depends on the stiffness of the lever (i.e., the free-running frequency) and the width of the resonance envelope. The latter is severely degraded in water, and soft levers are preferred for analysis of live cells. Although resonance mode imaging has many advantages, the jury is probably still out in the case of in vitro analysis of cells ***(9–11)***.

3.2.3. Analysis of Cell Dynamics

As mentioned in **Subheading 1.**, the AFM is uniquely capable of tracking the temporal evolution of systems consisting of living cells in a biocompatible fluid. There are distinctly different methodologies for slow (>10 min) and fast (<10 min) dynamics.

3.2.3.1. Slow Dynamics

A skilled operator can establish good imaging conditions within a few minutes. The acquisition of an image takes typically 1–3 min. Thus, sequential imaging over a particular field of view can track cell dynamics in vitro on the time scale of some minutes. As in the cases described in **Subheading 3.1.2.**, a soft lever (k_N < 0.01 N/m) in combination with a low applied force (<1 nN) will enhance information arising from the softer elements of the cell, whereas a stiffer lever and greater applied force will deform the plasma membrane and enhance visualization of the less compressible cytoskeletal and intracellular structures. The more informative studies have exploited the latter strategy to gain insight into cytoskeletal dynamics (e.g., **refs. *5,12–14***). An example of investigations of slow intracellular dynamics is shown in a sequence of images in **Fig. 3,** where the intracellular nucleation and growth over a period of 3 h of formazan crystals is apparent. The crystals arise from enzymatic conversion of a tetrazolium salt during the MTT (3-[4,5-dimethyl thiazol-2-yl]-2,5-diphenyl tetrazolium bromide) assay of viable cells ***(5)***.

3.2.3.2. Fast Dynamics

Biological activity on the sub-second time scale can be observed and analyzed by AFM methodologies by monitoring the deflection of a lever stationary in the *x–y* plane and sensed effectively in the constant height mode (i.e., where the time-constant of the feedback loop is longer than that of the biological response mechanism). The tip is simply landed at an appropriate location predetermined from an image. The *x–y* scan function is deactivated, and the dynamic response is monitored through the *z* deflection of the lever. A soft lever is most appropriate because the probe is ideally a passive participant in the temporal evolution. The method has been deployed with considerable success in the case of cardiomyocytes ***(15,16)***. There is clearly considerable scope for applications of similar methodologies for investigations of other manifestations of cellular dynamics.

3.2.4. Analysis of Mechanical Properties

3.2.4.1. F-d Measurements

The interaction between a tip and a surface is a function of the force imposed by the lever and manifests itself as a force acting on the tip while being sensed

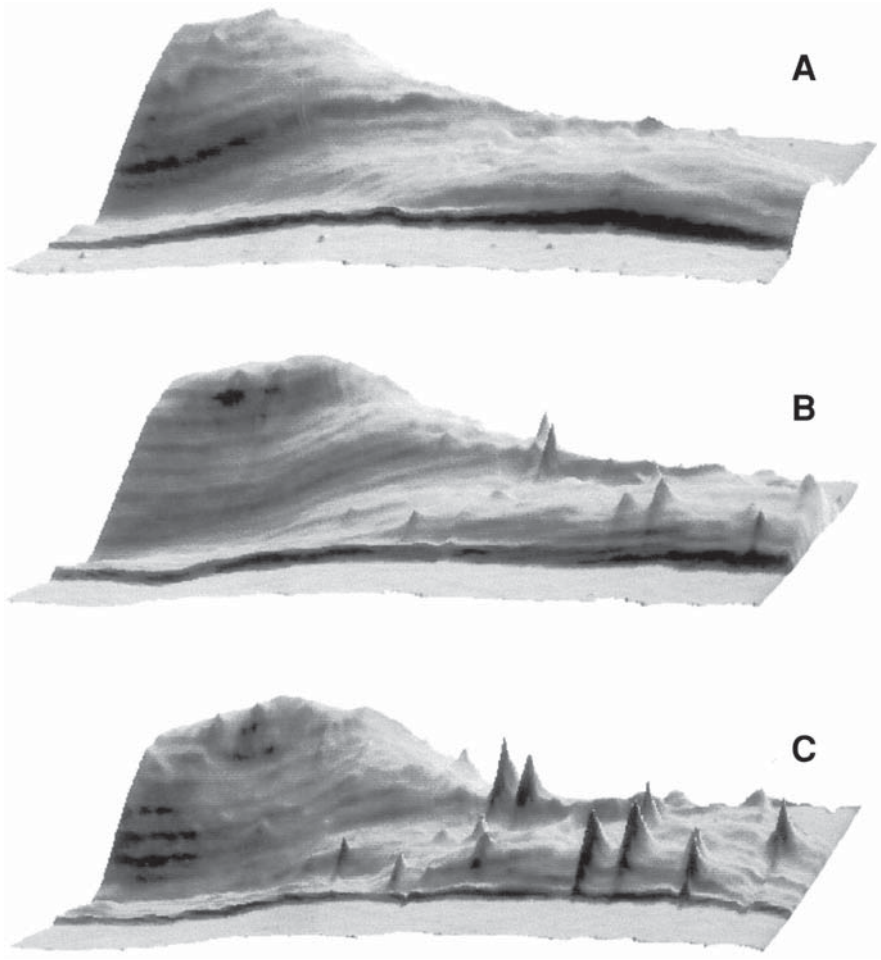

Fig. 3. Sequence of contact mode images from a lamellipodial region obtained in vitro showing nucleation and growth of formazan crystals within a viable cell. Images acquired after **(A)** 30 min; **(B)** 90 min; **(C)** 180 min.

by the lever. Such a system consists of two compliant elements–the lever and the surface–whereas all other components of the system are assumed to be rigid. Thus, compressional forces will cause bending of the lever and indentation of the surface by the tip. If the shape of the tip, the spring constant of the lever, the applied force, and the depth of indentation are known, then an effective Young's modulus for the surface can be calculated. Characteristic features of an F-d curve in combination with measurements of z stage travel and lever deflection allow such calculations to be conducted. The details of the proce-

dure have been described elsewhere (e.g., **refs. *5,17,18***). Adhesion between tip and surface manifests itself as an attractive force, causing deflection of the lever at the point of lift-off in the F-d curve. Because the strength of adhesion is a reflection of the local surface chemistry, then mapping of the surface adhesion of living cells may provide valuable additional information.

3.2.4.2. F-d Methodology for Fibroblasts

The effective Young's modulus of a supported section of the plasma membrane is in the range 1–10 kPa, whereas the corresponding value for a membrane more strongly supported by the cytoskeletal structure is in the range 15–50 kPa. The effective modulus of fixed cells is an order of magnitude higher ***(5,19)***. To obtain reliable information about mechanical properties, it is necessary that the spring constant of the lever be comparable with the effective force constant of interaction between tip and specimen. Thus, k_N in the range 0.01 N/m must be chosen. Given the extreme softness of the plasma membrane there is no incentive for working with sharp tips; even lever-imposed forces in the sub-nN range will give rise to tip indentations of 2–40 nm and contact areas of greater than 100 nm^2. Adhesive interactions add to the lever-imposed force and cause additional indentation and yet greater contact area.

3.3. Generic Outcomes of F-d Analysis of Live Fibroblasts

The results in **Fig. 4** illustrate typical outcomes of F-d analysis in vitro of fibroblasts. A standard probe with k_N = 0.03 N/m and a pyramidal tip shape, nominal radius of curvature of 40 nm, and an aspect ratio of 0.7 was used for the measurements. The data illustrate tip indentation, differences in stiffness measured at different locations, **a** and **b,** on the plasma membrane, the relative incompressibility of a fixed cell, and adhesive interactions between tip and membrane. The horizontal axis refers to *z*-stage travel, whereas the vertical axis shows lever deflection in the *z* direction.

3.4. Summary of AFM Studies Conducted on Fibroblasts

Table 1 summarizes critical methodological aspects of earlier AFM-based studies of flbroblasts and provides references for additional information.

4. Notes

1. Cell adhesion to substrate. Cell adhesion remains a significant methodological issue, although treated tissue culture substrates will generally offer acceptable performance. The extent of adhesion can readily be ascertained by running single line scans repetitively over a representative part of a cell. In extreme circumstances, a line scan will remove the entire cell from its substrate. The reproducibility of features in successive line scans is a useful monitor of stability of the

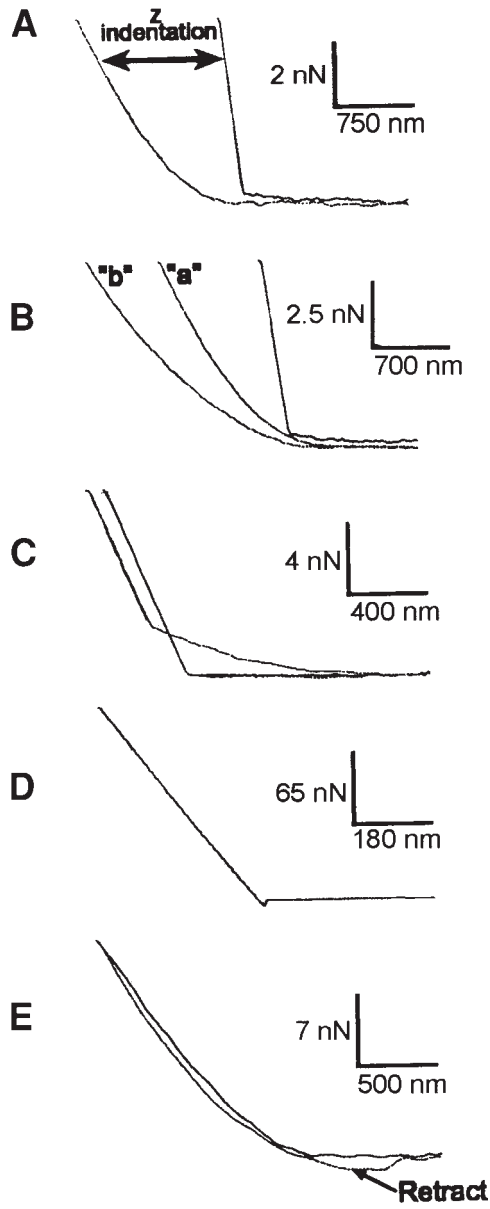

Fig. 4. **(A)** F-d curves obtained in vitro for a live flbroblast for different conditions. The steeper curve shows deflection of the lever by an incompressible surface and was used to calibrate the detector (relating nA difference current to lever deflection in nm). The less steep nonlinear curve reflects indentation by the tip in a compressible surface (i.e., the plasma membrane). In **(B)** are shown a calibration curve and the results of indenting a soft, **b**, and a stiffer, **a**, region of the plasma membrane. The data in **(C)**

Table 1
Methodological Aspects of Past Studies of Fibroblasts

Cell type	Substrate	Subst. coating	AFM mode	Probe(s)	Ref.
Fibroblasts, etc.	Glass cover slip	None	Contact	$Si_3N_4 k_N$ = 0.0 1,0.03	***20***
L929	Culture dish	None	Contact, F-d	$Si_3N_4 k_N$ = 0.03,0.06	***21***
Fibroblasts, etc.	Plastic dish	None	Contact	$Si_3N_4 k_N$ = 0.03	***13***
3T3	Plastic dish	None	Contact, F-d	$Si_3N_4 k_N$ = 0.08	***22***
3T6	Glass cover slip	None	Contact, F-d	$Si_3N_4 k_N$ = 0.01	***23***
3T3, NRK	Plastic dish	None	Contact, F-d	$Si_3N_4 k_N$ = 0.08	***14***
NIH3T3	Glass dish	Fibronectin	Contact, F-d	$Si_3N_4 k_N$ = 0.018	***24***
NIH3T3	Glass dish	Fibronectin	Contact, F-d(m)[a]	$Si_3N_4 k_N$ = 0.03	***25***

[a]A viscoelastic modulation method was adopted for the particular study.

cell during actual imaging conditions, as well as providing a measure of nondestructiveness of tip–cell interactions. Optimum quality of the image can also be obtained through adjustments of fast-scan speed and direction, force loading, parameters of the feedback loop, and field of view.

2. Tip contamination: effects and diagnostics. A cell cultured in a biofluid contains proteins, cell debris, and other contaminants in solution. The probe tip will inevitably become contaminated, at the very least, by nonspecific adsorption of proteins. Biofouling of the tip will alter the surface chemistry of the tip, and thus potentially its a destructive adherence to the cell, as well as its topography, with consequential degradation in resolution. The latter is not a serious problem, in the case of biomolecular adsorption, since extreme lateral resolution is not

---

Fig. 4. *(continued)* show that under compression the hard substrate will finally provide support for the cellular structures being compressed. The data in **(D)** demonstrate that fixing has the effect of making the cell more rigid; the cell is now effectively incompressible while the lever is the only compliant element. In **(E)** are shown both approach and retract half-cycles for a biofouled tip being used to analyze a cell. The adhesive interaction in the retract curve should be noted. Lever deflection for all curves can readily be converted to force applied, or sensed, by the lever by multiplying Z_L by k_N.

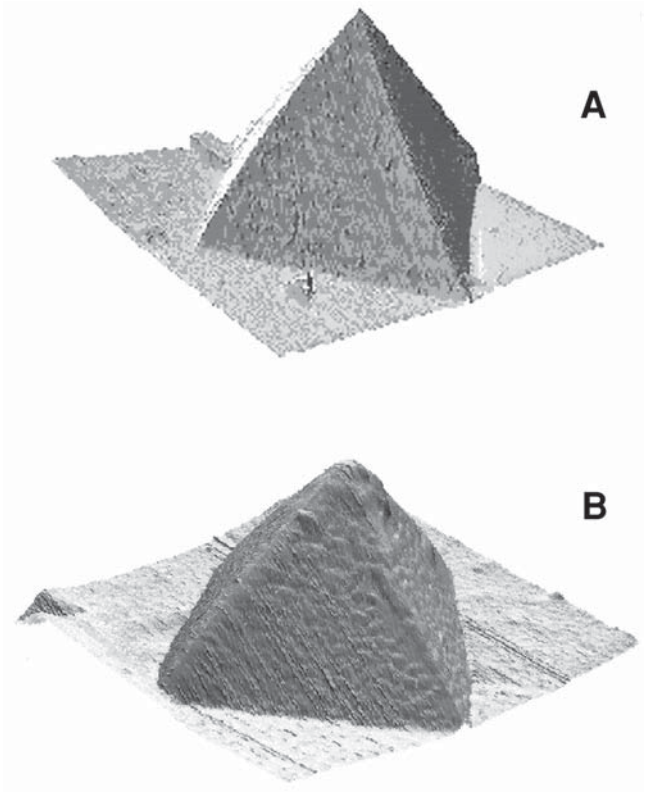

Fig. 5. Reverse images of a probe as-received **(A)** and after exposure to a biofluid **(B)**.

obtainable in any case because of the large contact area of the tip with the deformable plasma membrane. Cell debris attaching itself to the tip, however, has the effect of reducing image resolution, often to the point of complete obliteration. Here are several ways of diagnosing tip fouling, aside from its effect on the image quality. Because the general topography of the substrate can be determined at any time with a fresh tip, any subsequent deterioration in definition of topographical resolution must be caused by tip fouling. A more quantitative method is to conduct reverse imaging of the tip ***(8,26)***, whereby an image of the tip is generated from a scan over a spiky feature (e.g., an upturned tip attached to a substrate). **Figure 5** shows reverse images of an as-received tip, and of a tip after exposure to a biofluid. Finally, a contaminated tip may be analyzed in the F-d mode by indenting on a known hard substrate. If the tip is compliant, as a result of adherent biodebris, then it will be obvious from the F-d curves.

3. Common image artifacts. Several of the early studies have reported prominent effects because of precipitation of salts from the biofluid solution. If the analysis

is conducted in an open cell, and the cell is subject to evaporative losses, then the solution will become supersaturated in salts. Consequently, crystalline precipitates will form within the field of view. Moreover, the biofluid will no longer be compatible with cell viability. Frequent replacement of the biofluid will substantially eliminate that problem.

Tip-broadening and other tip-related artifacts will occur when the actual topography of the object being imaged is defined by radii of curvature less than or comparable to the radius of curvature of the tip, and/or when there are gradients exceeding that corresponding to the aspect ratio of the tip. For instance, images of tobacco mosaic virus (TMV) attached to a flat substrate obtained by AFM reveal the correct height of approx 18 nm, but the apparent lateral width will be in the range 60–100 nm as a result of the tip-shape convolution ***(27)***. Because the radius of the cylindrical TMV is known and is comparable to that of the apex of the tip, the apparent width of the object, *W*, in is given by the following:

$$W = 2[(R_{\mathrm{TMV}} + R_{\mathrm{Tip}})^2 - (R_{\mathrm{Tip}} - \mathrm{R}_{\mathrm{TMV}})^2]^{1/2}$$

When cytoskeletal structure is being imaged, the situation is somewhat more complicated by filamentary objects located some distance above the substrate. The aspect ratio then comes into play because the deformable membrane allows the tip to indent the cell on either side of the filamentary object. The apparent width will now depend on the height, *h*, of the object above the point of greatest indentation by the tip on either side of the object. The relevant expression is now as follows:

$$W \approx 2[hA_{\mathrm{r}}^{-1} + (r_{\mathrm{tip}} + r_{\mathrm{obj}})\cos\,\phi]$$

where the radii of the tip and object are r_{tip} and r_{obj}, respectively; A_{r}, is the aspect ratio of the tip, and the angle is defined by $\phi = \tan^{-1} A_{\mathrm{r}}^{-1}$.

Finally, other grosser artifacts will occur when the dynamic range of the *z* stage is exceeded; the image then becomes entirely featureless. A similar effect occurs when the *z*-height corrugations of the object exceed the height of the tip, and the surface of the lever defines the point of contact. The interaction is no longer localized, and the details of the image become washed out. Likewise, F-d analysis will now produce erroneous data since the spring constant will depend on an unknown and changing point of contact and the contact area will also be much greater leading to erroneous conclusions about indentation and adhesion.

Acknowledgments

Some of the work described above was funded in part by the Australian Research Council.

References

1. Gould, S. A. C., Drake, B., Prater, C. B., Weisenhorn, A. L., Manne, S., Hansma, H. G., et al. (1990) From atoms to integrated-circuit chips, blood-cells, and bacteria with the atomic force microscope. *J. Vac. Sci. Technol. A* **8,** 369–373.

2. Henderson, E., Haydon, P. G., and Sakaguchi, D. S. (1992) Actin filament dynamics in living glial cells imaged by atomic force microscopy. *Science* **257,** 1944–1946.
3. Hoh, J. H. and Hansma, P. K. (1992) Atomic force microscopy for high-resolution imaging in cell biology. *Trends Cell Biol.* **2,** 208–212.
4. Hong, X. and Lei, Y. (1999) Atomic force microscopy of living cells: progress, problems and prospects. *Methods Cell Sci.* **21,** 1–17.
5. Bushell, G. R., Cahill, C., Clarke, F. M, Gibson, C. T., Myhra, S., and Watson, G. S. (1999) Imaging and force-distance analysis of human fibroblasts in vitro by atomic force microscopy. *Cytometry* **36,** 254–264.
6. Pietrasanta, L. I., Schaper, A., and Jovin, T. M. (1994) Imaging subcellular structures of rat mammary carcinoma cells by scanning force microscopy. *J. Cell Sci.* **107,** 2427–2437.
7. Gibson, C. T., Watson, G. S., and Myhra, S. (1996) Determination of the spring constants of probes for force microscopy/spectroscopy. *Nanotechnology* **7,** 259–262.
8. Gibson, C. T., Watson, G. S., and Myhra, S. (1997) Scanning force microscopy - calibrative procedures for 'best practice'. *Scanning* **19,** 564–581.
9. Putman, C. A. J., van der Werf, K. O., de Grooth, B. G., van Hulst, N. F., and Greve, J. (1994) Viscoelsticity of living cells allows high resolution imaging by tapping mode atomic force microscopy. *Biophys. J.* **67,**1749–1753.
10. Le Grimellec, C., Lesniewska, E., Giocondi, M.-C., Finot, E., and Goudonnet, J.-P. (1997) Simultaneous imaging of the surface and submembraneous cytoskeleton hi living cells by tapping mode atomic force microscopy. *Acad. Sci. Biophys.* **320,** 637–643.
11. Vie, V., Giocondi, M.-C., Lesniewska, E., Finot, E., Goudonnet, J.-P., and Le Grimellec, C. (2000) Tapping-mode atomic force microscopy on intact cells: optimal adjustment of tapping conditions by using the dflection signal. *Ultramicroscopy* **82,** 279–288.
12. Schoenenberger, C.-A., and Hoh, J. H. (1994) Slow cellular dynamics in MDCK and R5 cells monitored by time-lapse atomic force microscopy. *Biophys. J.* **67,** 929–936.
13. Braet, F., Saynaeve, C., de Zanger, R., and Wisse, E. (1998) Imaging surface and submembraneous structures with the atomic force microscope: a study on living cancer cells, fibroblasts and macrophages. *J. Microsc.* **190,** 328–338.
14. Rotsch, C. and Radmacher, M. (2000) Drug-induced changes of cytoskeletal structure and mechanics in fibroblasts: an atomic force microscopy study. *Biophys. J.* **78,** 520–535.
15. Shroff, S. G., Saner, D. R., and Lai, R. (1995) Dynamic micromechanical properties of cultured rat atrial myocytes measured by atomic force microscopy. *Am. J. Physiol.* **269,** C286–C292.
16. Domke, J., Parak, W. J., George, M., Gaub, H. E., and Radmacher, M. (1999) Mapping the mechanical pulse of single cardiomyocytes with the atomic force microscope. *Eur. Biophys. J.* **28,**179–186.

17. Crossley, J. A. A., Gibson, C. T., Mapledoram, L. D., Huson, M. G., Myhra, S., Pham, D. K., et al. (2000) Atomic force microscopy analysis of wool fibre surfaces in air and under water. *Micron* **31,** 659–667.
18. Blach, J., Loughlin, W., Watson, G., and Myhra, S. (2001) Surface characterization of human hair by atomic force microscopy in the imaging and F-d modes. *Int. J. Cosm. Sci.* **23,**165–174.
19. Wu, H. W., Kuhn, T., and Moy, V. T. (1998) Mechanical properties of L929 cells measured by atomic force microscopy: effects of anticytoskeletal drugs and membrane crosslinking. *Scanning* **20,** 389–397.
20. Kuznetsov, Y. G., Malkin, A. J., and McPherson, A. (1997) Atomic force microscopy studies of living cells: Visualization of motility, division, aggregation, transformation and apoptosis. *J. Struct. Biol.* **120,**180–191.
21. Wu, H. W., Kuhn, T., and Moy, V. T. (1998) Mechanical properties of L929 cells measured by atomic force microscopy: effects of anticytoskeletal drugs and membrane crosslinking. *Scanning* **20,** 389–397.
22. Rotsch, C., Jacobson, K., and Radmacher, M. (1999) Dimensional and mechanical dynamics of active and stable edges in motile fibroblasts investigated by using atomic force microscopy. *Proc. Natl. Acad. Sci. USA* **96,** 921–926.
23. Ricci, D., Tedesco, M., and Grattarola, M. (1997) Mechanical and morphological properties of living 3T6 cells probed via scanning force microscopy. *Microsc. Res. Tech.* **36,** 165–171.
24. Haga, H., Sasaki, S., Kawabata, K., Ito, E., Ushiki, T., and Sambongi, T. (2000) Elasticity mapping of living fibroblasts by AFM and immunofluorescence observation of the cytoskeleton. *Ultramicroscopy* **82,** 253–258.
25. Haga, H., Nagayama., M., Kawabata, K., Ito, E., Ushiki, T., and Sambongi, T. (2000) Time-lapse viscoelastic imaging of living fibroblasts using force modulation in AFM. *J. Electron Microsc.* **49,** 473–481.
26. Hellemans, L., Waeyaert, K., and Hennau, F. (1991) Can atomic force microscopy tips be inspected by atomic force microscopy? *J. Vac. Sci. Technol.* **B9,** 1309–1312.
27. Bushell, G. R., Watson, G. S., Holt, S.A., and Myhra, S. (1995) Imaging and nano-dissection of tobacco mosaic virus by atomic force microscopy. *J. Microsc.* **180,**174–181.